

Possible Localized Modes in the Uniform Quantum Heisenberg Chains of Sr_2CuO_3 .

J.P. Boucher^{a,b} and M. Takigawa^c

^a *Laboratoire de Spectrométrie Physique, Université J. Fourier Grenoble I, BP 87, 38402 Saint Martin d'Hères cedex, France.*

^b *Department of Physics, Kyushu University 33, Fukuoka, 812-8581, Japan.*

^c *Institute for Solid State Physics, University of Tokyo, Roppongi, Minato-ku, Tokyo 106, Japan.*

(25 Septembre 1999)

A model of mobile bond-defects is tentatively proposed to analyze the “anomalies” observed on the NMR spectrum of the quantum Heisenberg chains of Sr_2CuO_3 . A bond-defect is a local change in the exchange coupling. It results in a local alternating magnetization (LAM), which, when the defect moves, creates a flipping process of the local field seen by each nuclear spin. At low temperature, when the overlap of the LAM becomes large, the defects form a periodic structure, which extends over almost all the chains. In that regime, the density of bond-defects decreases linearly with T .

75.20Hr; 76.60.-k

In low-dimensional quantum antiferromagnets, the effects of impurities or defects in “gapped” and “un-gapped” systems may display drastic differences but also common features [1]. A good example of the latter case is provided by the uniform quantum ($s = 1/2$) Heisenberg chains (UQHC). Hereafter, we consider the effects due to defects in such systems. A “defect” is defined as a local change in the magnetic bond coupling. As the translational symmetry of the spin system is broken, a local alternating magnetization (LAM) develops around the defects in the direction of the applied field: this is one of the common features mentioned above [1]. Such a LAM is probed accurately by NMR [2] [3]. Our analysis relies on results obtained on the compound Sr_2CuO_3 [2]. In such a “real system”, the elastic coupling between the spins and the lattice cannot be ignored. It can result in a lattice distortion giving rise to the so-called spin-Peierls transition (at temperature T_{sp}) [4]. Dynamical effects on LAM structures can also be expected from such magneto-elastic couplings. In the dimerized (D) phase of a spin-Peierls system (SPS), i.e., for $T < T_{sp}$, the LAM induced by chain-end effects become mobile in the pure one-dimensional case [5]. In the “high-field” phase of a SPS, a periodic LAM structure occurs, which results from the field-induced incommensurate lattice modulation [6]. In that case, dynamical effects are due to the quantum fluctuations of the phason modes describing the vibrations of the modulated lattice structure [6]. In the uniform phase of a SPS, i.e. for $T > T_{sp}$, the spin-lattice coupling is also of crucial importance. It can appreciably change the magnetic susceptibility of the system well above T_{sp} [7].

In Sr_2CuO_3 , no spin-Peierls transition is observed as a 3-dimensional magnetic ordering takes place at $T_N \simeq 5$ K. Above T_N , this compound provides a remarkable example of UQHC. The exchange coupling is large ($J \simeq 2200$ K). The logarithmic corrections characterizing the quantum ($T \ll J$) behavior of UQHC have been observed [8]. LAM associated with the edges of finite chains

have also been observed in Sr_2CuO_3 [2]. Due to that LAM, the NMR lineshape is changed in a very specific way, giving rise to “features”, which have been well identified. This is the case of features “A” displayed in Figs. 1 and 2. Other features, however, are visible on the NMR line (features “B” and “C” in Figs. 1 and 2), which have not been explained yet. We propose an analysis of these additional features in terms of LAM associated with mobile “bond-defects”.

The NMR spectra to be analyzed - a few examples are displayed in Figs. 1 and 2 - have been obtained on an Ar-annealed single crystal. That annealing procedure minimizes in that compound the possible source of impurities induced by interstitial excess oxygen. After such a treatment, the concentration of the residual spin-1/2 impurities becomes as low as $1.3 \cdot 10^{-4}$ [8]. Some of the NMR spectra displayed in Figs. 1 and 2 have been previously reported (Figs. 1a, b and Fig. 2a) in [2] together with the experimental conditions. As clearly established in [2], features “A” originate from the chain edges, while we show here that features “B” is well explained by the presence of mobile bond-defects. Features “C” would result from the periodic structure they form at low T . Finally, possible origins of these defects are suggested in relation with the lattice properties.

First we consider features “A”. LAM associated with the edges of finite UQHC have been described by Egger and Affleck [9]. The LAM amplitude increases with distance from the chain end. At $T \neq 0$ however, thermal fluctuations act as a cutoff, and at long distance, the LAM amplitude decreases exponentially with a characteristic scale given by the correlation length of the system: $\xi = J/2T$. An analytical expression for the local susceptibility has been derived, which agrees well with Monte-Carlo calculations. Accordingly, for an hyperfine coupling A_β (expressed in GHz and $\beta = \mathbf{a}, \mathbf{b}$ or \mathbf{c} referring to the field direction with respect to the crystal axes - chain axis \mathbf{b}), the local field seen by a nuclear spin at site n (counted from a chain end) can be written

$$h_n = -(-1)^n B A_\beta H \{(n + \phi)/\sqrt{\xi \sinh(2(n + \phi)/\xi)} \quad (1)$$

with $B \simeq 0.020 \text{ GHz}^{-1}$ and h_n and H expressed in Tesla. In (1), ϕ allows for a small shift of the LAM along the chain. ϕ changes the position n_{max} (see Fig. 3a) of the maximum field value, but for $\phi \leq n_{max}$, it does not affect this value: $h_{max} \simeq 1.08 \cdot 10^{-2} A_\beta H \sqrt{\xi}$ ($A_a \simeq 0.14 \text{ GHz}$ and $A_c \simeq 0.50 \text{ GHz}$). In the NMR spectrum, the field splitting ΔH (see Fig. 1) where features “A” occur is given by $\Delta H = 2h_{max}$. In that respect, as explained in [2], a very good agreement is obtained between theory and experiment. The shape of features “A”, however, depends appreciably on ϕ (see dot line $\phi = 0$ in Fig. 1b). Using ϕ as an adjustable parameter, a good agreement with the experimental line shape can be achieved for all the collected data (see dots in Figs. 1 and 2). With that procedure, one obtains that ϕ is field independent. It shows, however, a T dependence: $\phi = (1200 \pm 200)/T$, which, remarkably, agrees with $\phi \simeq \xi$. As shown in Fig. 3a (solid line), for that particular value of ϕ , the LAM displays no maximum, but a rather “flat” initial behavior. Despite the rough description used here, one is led to conclude that the initial increase of the LAM amplitude is not observed experimentally, in contradiction with the theoretical prediction [9]. The elastic spin-lattice coupling may play here an important role. The model of a sudden cutoff of the exchange coupling ($J = 0$) just at the chain edges would not applied to such “real” systems. Instead, as in the D phase of a SPS [10], on a length scale $\simeq \xi$, a distribution of the J-bonds would take place, giving rise to the observed “smoothing” of the initial LAM amplitude.

Second, we consider features “B”. We assume that they result from a local change in the exchange coupling ($J' \neq J$). As studied by Eggert (for $J' < J$) [11], LAM similar to the case $J' = 0$ develop around such bond-defects. We suppose that the associated LAM can be described by an expression similar to (1), but with a multiplying factor α ($\alpha < 1$) to account for the expected smaller amplitude. As before, a parameter ϕ' describes a possible “smoothing” effect around the defect position. Finally, we allow these defects to move along the chains. This dynamical behavior is of crucial importance for the NMR lineshape as it results in a “flipping” process of the hyperfine local field h'_n seen by the nuclear spins. Accordingly, the NMR signal of each nuclear spin is composed of 1 or 2 distinct lines depending on the flipping rate G with respect to the local hyperfine field h'_n . That “motional narrowing” is described as follows. For a nuclear spin at site n in the chain, the NMR spectrum is written

$$I_n = [D_0 + K'(\nu)] / \left\{ [\nu + K''(\nu)]^2 + D_0^2 + K'(\nu)^2 \right\} \quad (2)$$

with $K'(\nu) = \text{Re}\{K(\nu)\}$, $K''(\nu) = \text{Im}\{K(\nu)\}$ and $\nu = \nu^0 - \gamma H/2\pi$, where ν^0 is the experimental frequency and D_0 is the “natural” NMR width. $K(\nu)$ describes the effect of the dynamical local field as $K(\nu) =$

$(\gamma h'_n/2\pi)^2 k(\nu)$. Here, $k(\nu)$ is the Laplace representation of $k(t)$ which, as a function of time t , describes the flipping process due to the motion of the defects. A ballistic motion results in a linear exponential, $k(t) = \exp(-t/G)$, while a diffusive behavior gives $k(t) = \exp(-\sqrt{t/G})$ [12]. Such a single moving defect in a long chain may create additional “features” in the total NMR line, i.e., $I = \sum_n I_n$. That model allows us to reproduce very well the observed features “B”. An example is given in Fig. 3b, where a comparison with the data obtained for $H // \mathbf{a}$, at $\nu^0 = 87 \cdot 10^{-3} \text{ GHz}$ and $T = 30 \text{ K}$ is presented. The left side corresponds to a diffusive behavior with the parameters: $\phi' = 20$, $\alpha = 0.6$, $G = 2.8 \cdot 10^{-4} \text{ GHz}$ and $D_0 = 1.5 \cdot 10^{-5} \text{ GHz}$. The ballistic model (right side) gives usually a slightly poorer agreement (here with $\alpha = 0.45$, $G = 1.5 \cdot 10^{-4} \text{ GHz}$). That procedure applied to the different experimental conditions yields an interesting result concerning ϕ' . This parameter is independent on H , but it depends on T according to $\phi' = (600 \pm 100)/T \simeq \xi/2$. As for ϕ , this smoothing effect can be assumed to result from a local induced lattice distortion around the bond-defects.

In presence of several such bond-defects, the above description applies as long as the average distance between the defects remains large compared to ξ , i.e., a model of independent defects. At low T , however, interactions between defects are expected: a magnetic interaction should result from the overlap of the LAM structures and an elastic interaction from the lattice distortion associated with the defects. As a balance between these two interactions, we assume now that the defects form a periodic structure. If it is the case, the shape of the resulting LAM will depend on the number l of spins between two neighboring bond-defects. From the dashed line in Fig. 3a, approximate descriptions of such a LAM are represented in Fig. 3c, for l odd and even, respectively. As expected, for l even, a node occurs at the middle position. For l odd, the LAM amplitude remains finite at all positions. In the former case, the resulting NMR line displays a single narrow peak (Fig. 3d, right side). In the latter case, however, as the local field seen by the nuclear spins never cancels, a double structure develops at the centre of the NMR line (left side). For $H // \mathbf{a}$, in particular (see Fig. 1), such a central double structure is clearly observed below 30 K (and well reproduced by our model). For $H // \mathbf{c}$, the NMR line observed at $T = 30 \text{ K}$ (Fig. 2a) is more complex. In addition to the overlap of the three components of the quadrupolar splitting [2], it can be analyzed as composed of two contributions as illustrated in Fig. 2b. For one contribution (the dotted line), each component displays a narrow central peak (similar to the case described in Fig. 3d, right, for l even) and for the other, it displays a central double structure (as in Fig. 3d, left, for l odd). At lower T , however, only the double peak structure (features “C”) remains (see Fig. 2c). The contribution from segments

with l even is seen to decrease rapidly with T , and one is led to conclude that a periodic structure with l odd becomes energetically preferable.

A complete description of the NMR line at low T can now be proposed. A chain of N spins is considered, which contains a number η of bond-defects forming a periodic LAM structure with l odd. The dynamical behavior, i.e., the function $K(\nu)$ in Eq. 2, is now to be considered as describing the dynamics (or the thermal fluctuations) of that whole periodic LAM structure [13]. To account for the additional static local fields induced by the chain edges, expressions for h_n and h_{N-n} [given by Eq. (1)] are added to the applied field H in Eq. 2. The total NMR line, $I = \sum_n I_n$, is then calculated by varying the parameters α , G , l and D_0 . The parameters α and G are used to adjust the width of feature “B”. The shape of feature “C” is then determined by varying l and D_0 , keeping in mind that the narrowing effect, i.e., the parameter G , plays here a crucial role on the occurrence or not of such a small splitting at the centre of the NMR line. Finally the number η of bond-defects (with the condition $\eta l < N$) is used to adjust the intensity of features “A” relatively to that of the main line. With that procedure, one obtains the open dots in Figs. 1 and 2. The agreement with the experiments is in general excellent. Particular confidence in this approach is provided by the high sensitivity of the final agreement to only a few parameters, essentially l and G (compare the different lines in Fig. 3d, left). At low temperature, when features “C” are clearly visible, one always obtains the following determination: $\eta l \simeq N$ ($\simeq 1800 \pm 200$). This means that the periodic LAM structure develops practically over all the chain length. In that case, an evaluation of the density of the bond-defects is simply given by $\rho \simeq l^{-1}$. For $H // \mathbf{a}$, one obtains a rather accurate determination of the parameters α and G . They do not depend appreciably on T and H : $\alpha = 0.60 \pm 0.04$, $G = (2.8 \pm 0.2) 10^{-4}$ GHz. For $H // \mathbf{c}$, the determination is much more uncertain ($\alpha \simeq 0.46$ and $G \simeq 4.2 10^{-4}$ GHz) as a small contribution with l even is ignored in our description [14]. The parameter D_0 remains also constant ($D_0 \simeq 1.5 10^{-5}$ GHz for $H // \mathbf{a}$, and $D_0 \simeq 5.6 10^{-5}$ GHz for $H // \mathbf{c}$), except at the lowest temperature ($\simeq 20$ K) where larger values (by a factor $\simeq 2$) provide a better agreement. At low T , however, the description represented in Fig. 3c becomes insufficient when the overlap of the LAM becomes very large. The main variation is finally observed on the density of bond-defects $\rho \simeq l^{-1}$, which decreases almost linearly with T . This result is well established for $H // \mathbf{a}$ (Fig. 2d). The values obtained for $H // \mathbf{c}$ are also shown in that figure, though they are more uncertain for the reason explained above [14]. A first question raised by the present description concerns the source of the bond-defects ($J' < J$). Are they related to the interstitial excess oxygen which characterizes that compound? There are two reasons to rule out that possibility. First,

at the lowest temperature, $T = 20$ K, the density of bond-defects ($\rho \simeq 2.8 10^{-3}$) remains more than ten times larger than the concentration of the residual spin-1/2 impurities ($\simeq 1.3 10^{-4}$) after annealing. Second, the observed T dependence of ρ tells us that the number of bond-defects is not a constant but it decreases with T . Remarkably, ρ is observed to decrease linearly with T , as does the inverse of the spin correlation length $\xi^{-1} \simeq 2T/J$. That last remark strongly supports our assumption that the bond-defects are an intrinsic property of the “real” spin chains in Sr_2CuO_3 .

In the spin-Peierls phenomenology - and a priori above T_N , Sr_2CuO_3 is a SPS in its U phase - the description of the lattice is usually considered in its linear approximation. The lattice modes are described by simple phonon branches (characteristic frequency ν_p) and the spin-lattice coupling is considered in its adiabatic limit ($\nu_p < J$) [4]. A more realistic description, however, should take into account the non-linear properties of the lattice. They may give rise to additional “localized” (and rather mobile) excitations (lattice solitons, for instance). In the case of uniform chains, one kind of such non-linear excitations are of particular interest: the so-called “localized modes” as defined in [15]. They correspond to local oscillations of atoms, at high frequency and with large amplitude (breather like). Their presence in the lattice of an antiferromagnetic chain would result in bond-defects as those discussed above [16]. Alternatively, if the SP phenomenology is considered in its non-adiabatic limit ($\nu_p > J$), non-linearities might be also expected from the spin-lattice coupling itself. In that case, as discussed recently, the SP transition, instead of being driven by a phonon softening, would be associated with a “critical” central peak [17], which usually signals the presence of non-linear excitations. Well above T_{sp} , could this effective non-linearity explain the presence of localized excitations? The present NMR results may provide the first evidence of magneto-elastic localized modes in UQHC. A recent numerical investigation of such bond-defects in UQHC [18] has already established the following results: i) the expected magnetic interactions between two (static) bond-defects are attractive, ii) a LAM structure with l odd is energetically more favorable, iii) the LAM amplitude of an l -even structure decreases rapidly at low temperature. All these results agree with our analysis of the NMR line. Together with the possible repulsive interactions due to the lattice, they reinforce our proposition that a periodic LAM structure takes place at low T in UQHC. At that point, it is worth reminding that a double-peak structure, similar to our features “C”, has been observed in the SPS CuGeO_3 [19] well above T_{sp} , i.e., in its U phase. Our conclusion is that the presence of a LAM structure is strongly supported by the NMR results. We propose a model - bond-defects and a periodic LAM structure - which explains both features “B” and “C” in an unique consistent model. That model deserves

certainly to be comforted experimentally and theoretically. For instance, the quasi-static periodic AF structure of the LAM could be observed by neutron diffraction. Any description of such a “real” UQHC should consider explicitly the subtle relations between the spins and the lattice.

One of us (JPB) thanks G. Uhrig and T. Ziman for illuminating discussions, and S. Miyashita and the authors of Ref. [18] for communicating their results. Y. Ajiro is acknowledged for his invitation at Kyushu University, and the Japan Society for the Promotion of Science for its financial support.

-
- [1] M. Laukamp et al., Phys. Rev. B **55**, 10755.
 - [2] M. Takigawa et al. Phys. Rev. B **55**, 14129 (1997).
 - [3] Y. Fagot-Revurat et al., Phys. Rev. Lett. **77**, 1861 (1996); M. Horvatic et al., Phys. Rev. Lett. **83**, 420 (1999); F. Tedoldi et al., Phys. Rev. Lett. **83**, 412 (1999).
 - [4] J.W. Bray et al., in *Extended Linear Chain Compounds*, edited by J.S. Miller (Plenum Press, New York, 1983) Vol.3, p. 353.
 - [5] P. Hansen et al., submitted to Phys. Rev. B, cond-mat/9805325.
 - [6] G.S. Uhrig et al., Europhys. Lett. **41**, 431 (1998); G.S. Uhrig et al., to appear in Phys. Rev. B, cond-mat/9902272.
 - [7] A.W. Sandvik et al., Phys. Rev. B **56**, 14510 (1997).
 - [8] N. Motoyama et al., Phys. Rev. Lett., **76**, 3212 (1996); M. Takigawa et al., Phys. Rev. Lett. **76**, 4612 (1996), M. Takigawa et al., Phys. Rev. B **56**, 13681 (1997).
 - [9] S. Eggert and J. Affleck, Phys. Rev. Lett., **75**, 934 (1995).
 - [10] D. Augier et al. cond-mat/9807265; D. Augier et al., cond-mat/9908134.
 - [11] S. Eggert, Ph.D. Thesis, University of British Columbia, Vancouver, 1994 (unpublished); S. Eggert and I. Affleck, Phys. Rev. B **46**, 10866 (1992). See also, C.L. Kane and M.P.A. Fisher, Phys. Rev. B **46**, 15233 (1992).
 - [12] J.P. Boucher et al., Phys. Rev. Lett. **48**, 431 (1982).
 - [13] Gaussian fluctuations can also be considered. Different values will be obtained for the parameters, but the general behavior will not change qualitatively.
 - [14] With both l odd and even, too many parameters enter the description to provide very reliable values.
 - [15] A.J. Sievers and S. Takeno, Phys. Rev. Lett. **61**, 970 (1988).
 - [16] In particular, we expect the exchange coupling to be locally reduced and according to [11], a value $\alpha \simeq 0.6$ corresponds to $J/J' \simeq 0.5$.
 - [17] C. Gros and R. Werner, Phys. Rev. B **58**, R14677 (1998).
 - [18] M. Nishino et al., preprint, cond-mat/9906426.
 - [19] Y. Fagot-Revurat, Thèse, Université J. Fourier-Grenoble I, 1998 (unpublished).

FIG. 1. NMR signals (solid lines) obtained at different frequencies ν^0 , for H // **a** compared to calculated values (open dots). “A”, “B” and “C” denote the “features” to be explained. In b), the dotted line describing feature “A” corresponds to $\phi = 0$, while the calculation is obtained with $\phi = \xi$ (see dotted and solid lines in Fig. 3a).

FIG. 2. a) NMR line for H // **c**. The inset shows the details of the central parts of the three hyperfine components. The open dots are calculated for a periodic LAM with l odd only. b) Example of a spectrum resulting from LAM with both l even (dotted) and odd (dashed line), with relative intensity 0.13. c) Comparison between calculation for l odd only (open dots) and experiment (solid line) obtained at $T = 20$ K. d) T dependence of the defect density ρ for a model of a periodic LAM structure with l odd. The dotted line is a linear fit with the data for H // **a**. The data for H // **c** are also shown (see text).

FIG. 3. a) Contour of the local field (in absolute value) as a function of the site number n apart from a bond defect: $Y = h'_n/(BA_\beta H)$ and ξ , α and ϕ are defined in text. b) Description of feature “B” by independent mobile bond-defects in the diffusive and ballistic models (lines with open dots) compared to experimental data (solid line). c) Contour of the local field between bond-defects with l odd and even as used in our calculations. d) NMR lineshapes resulting from periodic LAM with l odd and even: the solid lines are calculated for the experimental conditions of Fig. 1b, with $G = 2.8 \cdot 10^{-4}$ GHz for $l = 241$ (left) and $l = 240$ (right); the dotted ($G = 2.2 \cdot 10^{-4}$ GHz, same $l = 241$) and dashed ($l = 261$, same $G = 2.8 \cdot 10^{-4}$ GHz) lines illustrate the high sensitivity of these parameters on the final lineshape.

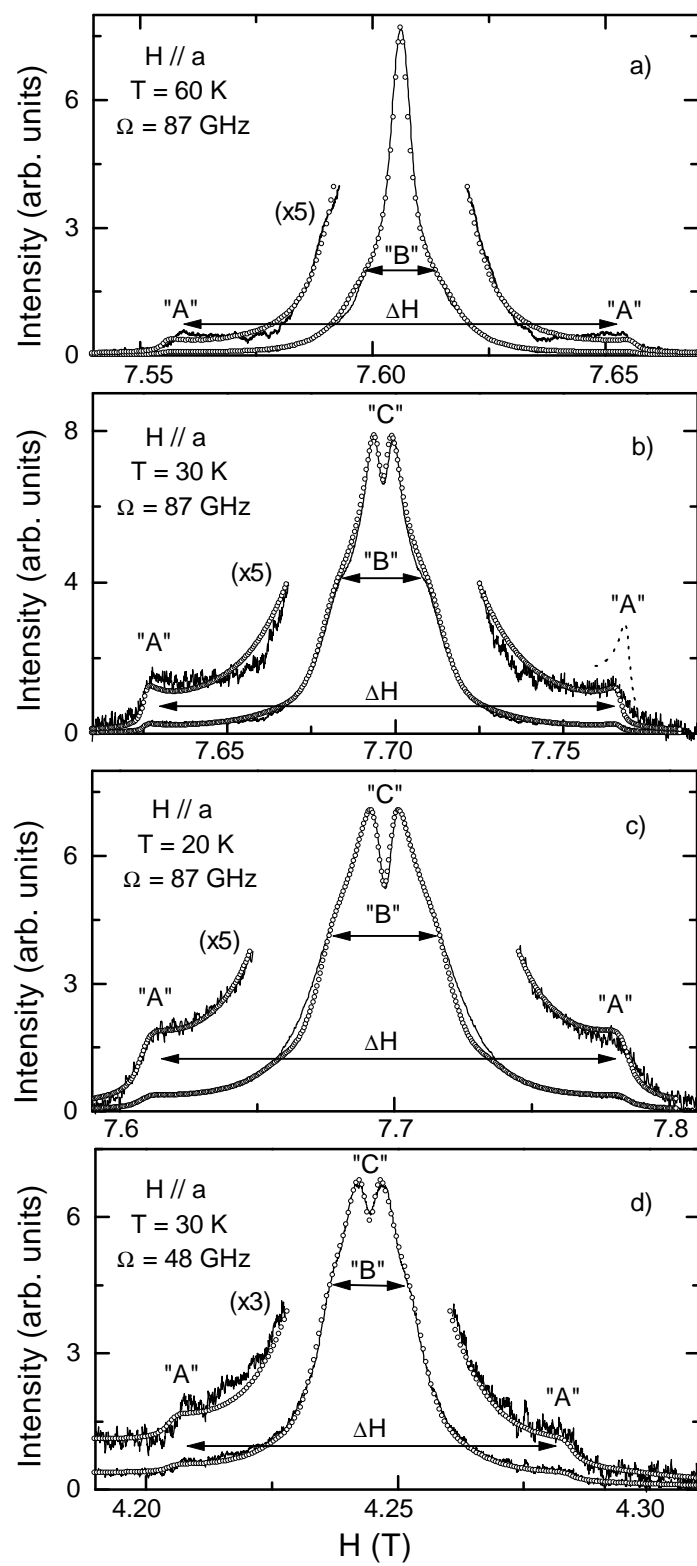


Fig.1

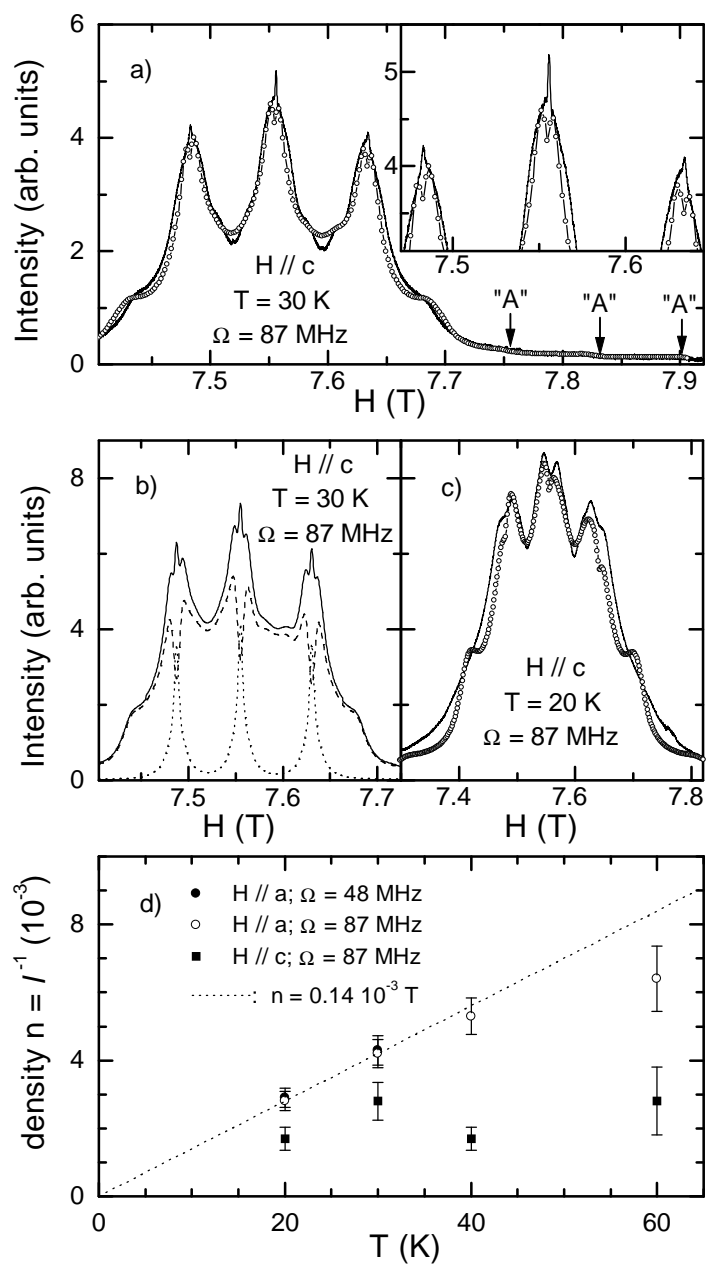


Fig.2

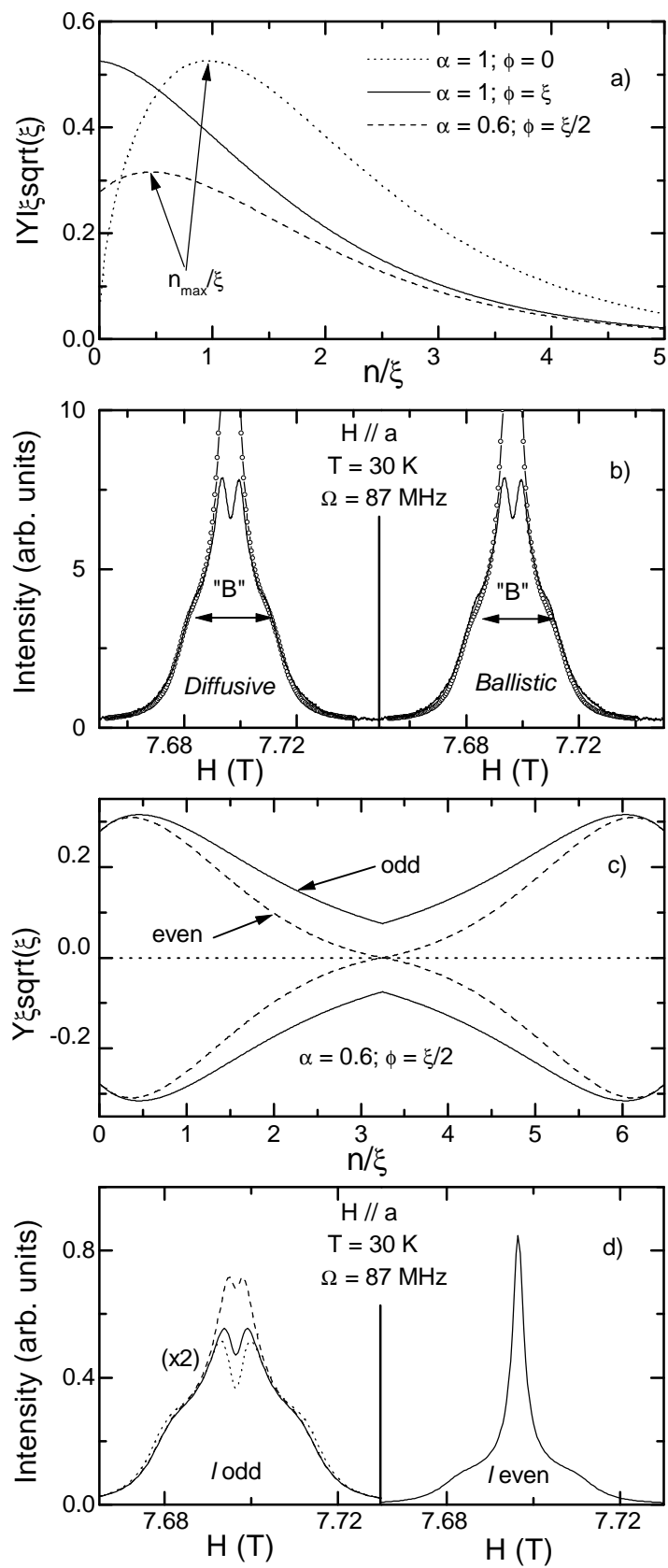


Fig.3